A Tunable Common Mode Inductor with an Auxiliary Winding Network

Danting Xu, Wai Man Ng, Sitthisak Kiratipongvoot, Chi Kwan Lee, Bryan M.H. Pong
Department of Electrical and Electronic Engineering
The University of Hong Kong
Hong Kong, China
Email: xudt@hku.hk

***Abstract*— In conventional switching converter, the parasitic capacitance between switching circuit and ground introduces common mode (CM) noise problem. A CM inductor is inserted in the power feeding paths to produce a high impedance to attenuate the CM noise. However, this parasitic capacitance and the CM inductor create low-frequency resonance near the switching frequency and its harmonics. Thus, the filtering performance is diminished. Increasing the CM inductance to shift the resonant frequency to low-frequency range is one of the methods to tackle this problem. However, this approach leads to increase the power losses (both core and winding losses) of the CM inductor reducing the efficiency of the converter. In this paper, a tunable CM inductor with a small-space auxiliary winding is proposed. The auxiliary winding can be connected to a passive network to alter the frequency response of the CM inductor without affecting the original inductance. As a result, the influence of the low-frequency resonance can be mitigated. A proof-of-concept protytpe is constructed and its performance is experimentally measured. Results show that the proposed tunable CM inductor operates as theoretically anticipated.**

Keywords—Common mode inductor; electromagnetic interference; filter component; tunable impedance

I. INTRODUCTION

Switching power converter generates electromagnetic interference (EMI) affecting the neighbor electronic products in normal operation. Over the past decade, numerous techniques such as EMI filtering, shielding, design optimization, etc are developed to tackle this problem. Passive EMI filtering technique is a common and effective solution to suppress EMI noise [1-3]. Stray and parasitic inductance and capacitance of the interconnection and filtering components reduce the effectiveness of the filter at high frequency. In order to eliminate this limitation, passive integrated EMI filter based on planar magnetic have been proposed to reduce the footprint area and stray components thus improve the frequency bandwidth [4-6]. Furthermore, coupled printed spiral windings (PSW) have also been applied to cancel the capacitor parasitic inductance in traditional EMI filters [7, 8]. In [9-11], hybrid EMI filter design has been proposed to replace conventional passive EMI filters. Since active filter offers good noise attenuation at a relatively low frequency band, hybrid concept combining both advantages of active and passive filter provides a good solution cover a wide frequency range.

The noise flowing between the power conversion system and the ground is usually called common mode (CM) noise and the noise flowing within the power feeding paths is usually called differential mode (DM) noise [12]. EMI filters which combining inductors and capacitors are usually used to attenuate both CM and DM noise as shown in Fig. 1. LISN is the line impedance stabilization network for conducted EMI test. The converter parasitic capacitance to the ground is highlighted in red color. We should note that that the paths of the CM noise signal flowing through the parasitic capacitance to the ground are invisible. Furthermore, it is difficult to determine the value of the parasitic capacitance. For instance, noise can pass thought the parasitic capacitance between the drain of the MOSFET and heat-sink or the parasitic capacitance between traces and the output load.

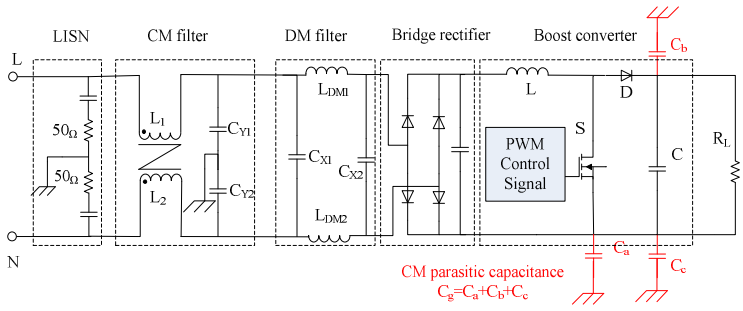

Fig. 1. EMI filter for a switching mode power supply.

The paper is organized as follows. In Section II, the CM noise model and the proposed tunable CM inductor will be introduced. The operating principle of the proposed CM inductor will be explicitly described using the corresponding equivalent circuit. Then, design procedure and passive components selection for the auxiliary windings will be analytically investigated and presented in Section III. Afterwards, the construction of a proof-of-concept prototype and its experimental measurement results will be discussed in Section IV. Section V gives the conclusions of the paper.

II. Circuit Analysis of CM Noise Model and Proposed CM Inductor

A. CM Noise Model

Fig. 2(a) shows an equivalent CM noise model of a switching mode power supply with a CM inductor, lumped CM capacitor and lumped parasitic capacitance. The CM noise source is denoted as V_g. C_g represents the total parasitic capacitance between the converter and ground. C_Y is the lumped Y capacitors of the CM filter. L_1 and L_2 are the self-inductance of the CM inductor. M is the mutual inductance between L_1 and L_2. C_{LISN} and R_{LISN} are the capacitance and resistance of the LISN, respectively. The CM noise model is further simplified using Thevinin's Theorem as shown in Fig. 2(b). The impedance looking into power feeding paths can be expressed as

$$Z_{in(Th)} = \frac{1}{sC_{Th}} + \frac{R_{LISN}}{2} + \frac{1}{s \times 2C_{LISN}} + \frac{s(L_1 + M)}{2} \quad (1)$$

where, $C_{Th}=C_Y+C_g$. The Thevinin's equivalent voltage V_{Th} is $V_{Th}=C_g/(C_Y+C_g)\times V_g$. The insertion loss of the CM noise filter can be obtained as

$$|Atten|_{dB} = 20\log_{10}\frac{V_{R_{LISN}}}{V_g} = 20\log_{10}\left(\frac{C_g}{(C_Y + C_g)} \times \frac{V_{R_{LISN}}}{V_{Th}}\right) \quad (2)$$
$$= 20\log_{10}\left(\frac{C_g}{(C_Y + C_g)} \times \frac{R_{LISN}}{2Z_{in(Th)}}\right)$$

In practical applications, the Y capacitor C_Y is limited by the maximum leakage current specified in the safety standard. In order to achieve enough attenuation of noise, the value of the CM inductor has to be large. The drawback of using a large value CM inductor is the low-frequency resonance created by the CM inductor and parasitic capacitance. Thus, the performance of the filter is poor around the resonant frequency.

In Fig. 3, the noise level at V_{R_LISN} (normalized to V_g) against the frequency with and without CM filter are plotted. The resonant frequency of the CM filter (in this example) is around 200 kHz. Modern switching converters are operated in hundreds of kilohertz up to megahertz. If the switching frequency of the converter is close to this resonant frequency, the noise current flowing within the power feeding paths could even be higher than without CM filter.

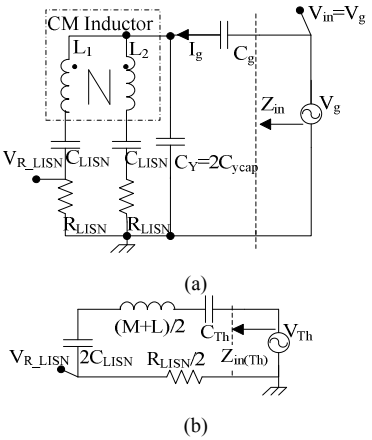

Fig. 2. (a) An equivalent CM noise model and (b) its Thevinin's equivalent circuit.

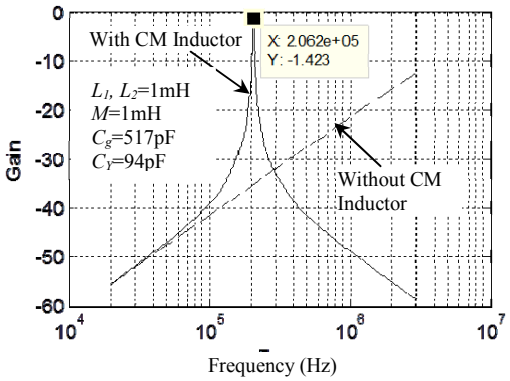

Fig. 3. Insertion loss of CM noise filter in Fig. 2

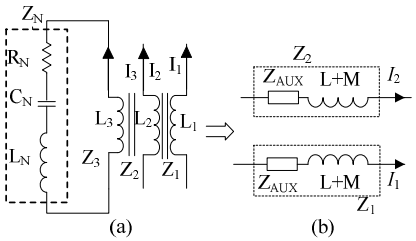

Fig. 4. (a) Schematic of the proposed tunable CM inductor and (b) its equivalent circuit in the CM noise model.

B. Proposed Tunable CM inductor

Fig. 4(a) depicts the schematic of the proposed tunable CM inductor with three coupled windings. L_1 and L_2 are the traditional CM inductor windings for power feeding paths. L_3 is an auxiliary winding which can be connected to an external impedance network (Z_N). The frequency response of the CM filter can be tuned by Z_N. The impedance equations for the coupled coils are expressed as

$$Z_1=\frac{V_1}{I_1}=sL_1+sM_{21}\frac{I_2}{I_1}+sM_{31}\frac{I_3}{I_1}$$
$$Z_2=\frac{V_2}{I_2}=sM_{12}\frac{I_1}{I_2}+sL_2+sM_{32}\frac{I_3}{I_2} \quad (3)$$
$$Z_3=\frac{V_3}{I_3}=sM_{13}\frac{I_1}{I_3}+sM_{23}\frac{I_2}{I_3}+sL_3$$

where, I_1, I_2, I_3 and V_1, V_2, V_3 are the corresponding CM noise current in and voltage across the L_1, L_2, and L_3, respectively. The windings are considered identically and tightly coupled. i.e. $M_{ij} = M$ (i,j=1,2,3i ≠ j) and $L_i = L$. CM current I_1 and I_2 are theoretically the same, so $I_1=I_2=I$. The impedance of Z_3 is

$$Z_3=\frac{V_3}{I_3}=-Z_N=2\times sM\times(\frac{I}{I_3})+sL. \quad (4)$$

Therefore,

$$\frac{I_3}{I}=\frac{2\times j\omega M}{-Z_N-j\omega L} \quad (5)$$

The impedance of Z_1 and Z_2 become

$$Z_1=Z_2=s(L+M)+Z_{AUX}. \quad (6)$$

where Z_{AUX} is $\frac{2\times s^2M^2}{-Z_N-sL}$ connected in-series with (L+M) as shown in Fig 4(b). And Z_{AUX} is a tunable complex impedance which can be implemented by using different impedance networks shaping the frequency response of the CM inductor. Further consider the windings are tightly coupled together. Therefore, $M=L$. Rewrite (6), the Z_1 and Z_2 can be expressed as

$$Z_1=Z_2=s(L+M)+\frac{2\times s^2M^2}{-Z_N-sL}=\frac{1}{\frac{1}{2\times Z_N}+\frac{1}{2\times sL}} \quad (7)$$

As a result, two impedance $2\times Z_N$ and $2\times sL$ are connected in parallel, i.e. $(2\times Z_N)//(2\times sL)$.

III. Components Selectrion and Tuning for the Tunable CM Inductor

A. Characteristics of Z_N

In this section, we discuss the characteristics of the tunable inductor based on the three basic components namely, resistor, inductor and capacitor.

Case 1. $Z_N = R_N$

Connecting a resistive element across the auxiliary winding, the insertion loss of the CM filter is plotted in Fig. 5. When R_N is small, the inductive property is diminished. The CM noise passes through the resistive element. As a result, R_N and C_{Th} forms a high pass filter. The cut-off frequency can be located at $W_c=1/(R_N\times C_{th})$. When R_N is large, the inductive property is dominated. The CM noise passes the auxiliary winding L_3. As a consequence, the behavior of the tunable CM

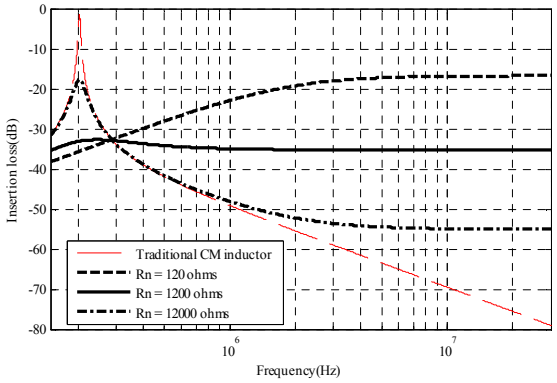

Fig. 5. Insertion loss at different R_N values in Matlab calculation

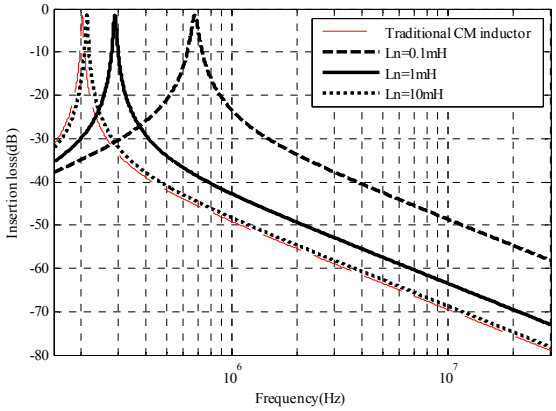

Fig. 6. Insertion loss at different L_N values in Matlab calculation

inductor is similar to the traditional CM inductor which has a low-frequency resonance at the low frequency range. However, R_N plays as a damping element in the resonant circuit to reduce the peak value at the resonant frequency. By choosing appropriate value of resistor R_N, the peak value of resonance could be controlled to balance the low- and high- frequency response of the CM filter. Therefore, the insertion loss in the both low and high frequency are similar.

Case 2. $Z_N = L_N$

In Fig. 6, the insertion loss of the CM filter with an inductor L_N connected across the auxiliary winding is plotted. It can be observed that L_N shifts the resonant frequency of the filter to higher frequency. It is because L_N is connected in parallel with the CM inductor. This property provides a freedom for the design engineer to adjust the resonant frequency of the CM filter. Practically, design engineer can relocates the resonant frequency of the CM filter to avoid the switching frequency and its harmonics of the switching power supply. However, this method will deteriorate the higher frequency noise attenuation because of the reduced total inductance of the CM filter.

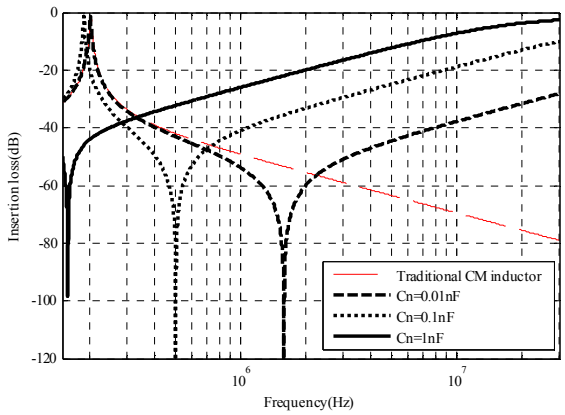

Fig. 7. Insertion loss at different C_N values in Matlab calculation

Case 3. $Z_N = C_N$

The insertion loss of the tunable CM inductor with a capacitor C_N connected across the auxiliary winding is plotted in Fig. 7. This capacitor would introduce a new zero for the system. In high frequency, the common mode inductors are 'shorted' by the capacitor and the high frequency is dominated by the capacitance in the circuit. The capacitor in auxiliary winding can introduce a zero to the circuit and by choosing C_N value, the zero would be used to cancel and suppress the resonance peak from the CM inductor. . But using this element has an obvious disadvantage that the high frequency performance is damaged by the capacitive element.

From the above discussion we conclude that using each case can get a corresponding outcome although they are not enough to cover the whole problem. For instance, R_N can damp the peak value but will make higher frequency worse; L_N can shift the peak to higher frequency a little bit so that the switching harmonics may be reduced but high frequency still has some attenuation loss; C_N can introduce a zero to cancel the original peak but may not work at high frequency.

B. Parameter selection

we now start to give a parameter selection method in which a series RLC circuit is chosen in Z_N network as a design example in Fig. 4 . In Fig. 8, an example is introduced to choose the Rn, Ln and Cn tep by step.

Step1. Select R_N

In this step, we add a resistor (Z_N=R_N) in the auxiliary winding then $Z'_{AUX} = \frac{2\times s^2 M^2}{-R_N - sL}$. Normally resistor is to reduce the Q factor and damp the resonance peak in resonant circuit. From (7) it is obvious that at and after the resonance frequency, the real part of the whole $Z'_{in(Th)}$ should become R_N and at the resonance the imaginary part of $Z'_{in(Th)}$ should be zero due to the definition of resonance frequency, and the total impedance for our noise model becomes $Z'_{in(Th)}$

$$Z'_{in(Th)} = real[Z'_{in(Th)}] + imag[Z'_{in(Th)}] \tag{8}$$

Equation (8) is an impedance decomposition for $Z'_{in(Th)}$ and it is easy to make $s=j\times w$ and get the real and imaginary part of $Z'_{in(Th)}$ respectively in (9) and (10),

$$real[Z'_{in(Th)}] = \frac{R}{2} + \frac{w^2\times M^2\times R_N}{R_N^2 + w^2\times L^2} \tag{9}$$

$$imag[Z'_{in(Th)}] = \frac{(L+M)\times w}{2} - \frac{1}{w\times Cth} - \frac{w^3\times M^2\times L}{R_N^2 + w^2\times L^2} \tag{10}$$

Theoretically at resonance frequency we make real[$Z'_{in(Th)}$] equal to Rn and imag[$Z'_{in(Th)}$] equal to 0 in (11),

$$\begin{aligned} real[Z'_{in(Th)}] &= R_N \\ imag[Z'_{in(Th)}] &= 0 \end{aligned} \tag{11}$$

So there will be two equations and two unknown variables, i.e. R_N and w' which is the resonant frequency, and we can get these two values. At this design stage we don't care about where the resonance happens because the parameter selection do not finish selecting yet, therefore we only take the R_N value as a parameter and it can be used at the other stage to select the other parameter. After selecting the R_N, the insertion loss of the noise model is shown in dotted line in Fig. 8.

Step 2. Select L_N

Resistor only affects real part of the total circuit impedance $Z_{in(Th)}$, adding a L_N value can shift the resonance peak to higher frequency band and may be designed independently without considering the R_N effect for this stage. Since L_N should not be too large in size, the high frequency band attenuation will decrease a little bit compared with the traditional CM filter. Assuming ΔdB is the acceptable loss for the attenuation, as shown in Fig. 6, it can be calculated as

$$\Delta dB = |Atten''|_{dB} - |Atten|_{dB} = 20\log_{10}\frac{|Z_{in(Th)}|}{|Z''_{in(Th)}|} \tag{12}$$

where $|Atten|_{dB}$ is the insertion loss for traditional CM filter and $|Atten|_{dB}''$ is the insertion loss after making Z_N=L_N, i.e $Z''_{AUX} = \frac{2\times s^2 M^2}{-sL_N - sL}$, and $Z''_{in(Th)}$ is the total impedance in the whole circuit.

Finally we get L_N value as:

$$L_N = \frac{s\times M^2}{[\frac{1}{s\times Cth} + \frac{1}{s\times 2\times C} + \frac{R}{2} + \frac{(L+M)}{2}\times s]\times(10^{\frac{\Delta dB}{20}} - 1)} - L \tag{13}$$

In our design, we only concern high frequency band, so by determining high frequency band (f≥25MHz) ΔdB(26dB in our design example) and solving (13) we can get L_N. . After

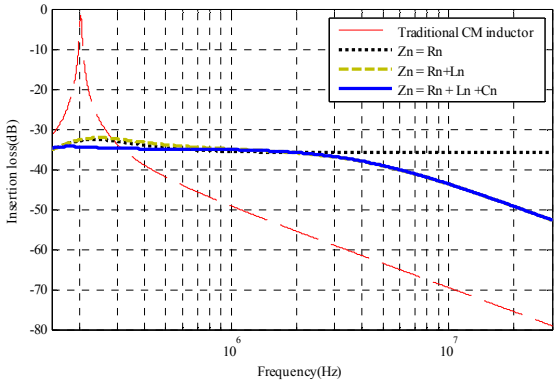

(a) Insertion loss after selecting parameters (150kHz to 30MHz)

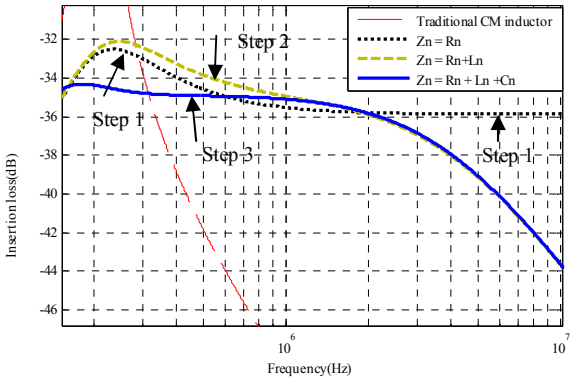

(b) Zoom in from 150 kHz to 10MHz

Fig. 8. (a)Insertion loss after selecting parameters step by step (b) Zoom in (150kHz-10MHz)

selecting the L_N, the insertion loss of the noise model is shown in dashed line in Fig. 8.

Step 3. Select C_N

Now we have R_N and L_N value for the network, the Z_{AUX} can be rewritten as $Z'''_{AUX} = \frac{-2s^2M^2}{(sL_N + R_N + 1/sC_N) + sL}$, so

$$Z'''_{in(Th)} = real[Z'''_{in(Th)}] + imag[Z'''_{in(Th)}] \qquad (14)$$

Similarly using the same method as selecting R_N, real[$Z'''_{in(Th)}$] equals to R_N and imag[$Z'''_{in(Th)}$] equal to 0 in (14) at resonant frequency respectively, so we can get C_N. After selecting the C_N, the insertion loss of the noise model is shown in solid line in Fig. 8.

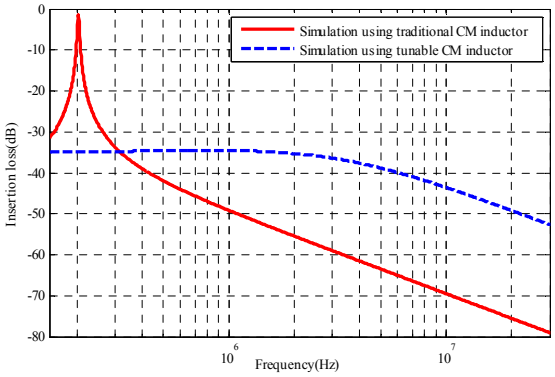

Fig. 9. Simulated insertion loss

By using this method in parameter selection procedure, R_N, L_N and C_N value are calculted as 1.29kΩ, 0.052mH and 1.26nF respectively. The simulation of insertion loss for the CM filter using and without using the proposed auxiliary winding results are evaluated by PSpice in Fig.9. It is important to note both results are almost the same in Fig. 9 and Fig. 8(a). However, the calculated and simulated results are based on the ideal components.

IV. VALIDATION

The CM noise model and the proposed tunable CM inductor prototype are built. Fig. 9 shows the setup of the experiment. The CM filter insertion loss is measured by using network analyzer, Agilen E5061B. The details components value of the LISN, CM capacitors, CM inductor and equivalent parasitic capacitor are summarized in Table I.

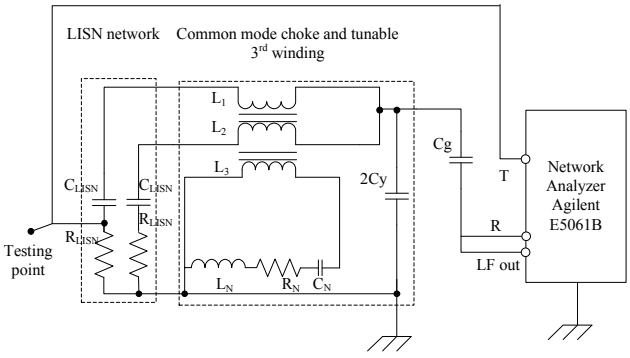

Fig. 10. Experiment setup

TABLE I. COMPONENTS VALUE OF THE CM NOISE MODEL AND CM INDUCTORS

LISN		Traditional CM Filter		Proposed CM inductor		Zn network	
C_{LISN}	0.1uF	L	1.026mH	L_1	903.1uH	R_N	1.2k
R_{LISN}	50ohms	M	984.1uH	L_2	905.2uH	C_N	1.4nF
C_g	517p	C_Y	47pF*2	L_3	966.1uH	L_N	0.05mH

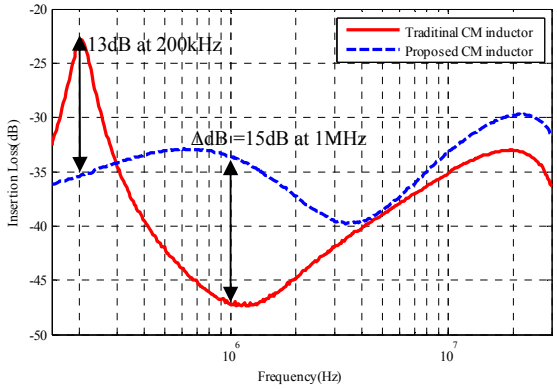

Fig. 11. Measured insertion loss

The measured insertion losses of CM filter with traditional and tunable CM inductors are plotted in Fig.11. By using the proposed CM inductor, the filter has a 13dB improvement at 200kHz. It also achieves over -30dB noise attenuation within 150kHz to 30MHz frequency range while the high frequency attenuation loss (ΔdB=15dB in experiment) which is not exactly the same as calculation and actually this value is much better than calculation result (ΔdB=26dB in calculation) but the trend is already predicted in design procedure The reason for the two different values is that the CM inductors have parasitic capacitance and will lead to self-resonance at around 1MHz thus fail to maintain the original inductive characteristic. Above all, both measurements and calculation results confirm that the proposed method can effectively eliminates the low frequency resonance.

The measured impedance and phase of the two CM inductors are shown in Fig. 12. It depicts that from 50Hz (line frequency) to around 10kHz, impedance and phase of the proposed inductor is the same with the traditional one, so the power dissipated on the inductor should be almost the same. From the phase characteristic in Fig. 12(b) it illustrates that the proposed tunable CM inductor has a wider inductive range than the traditional inductor, this is the reason that this tunable inductor can tune the insertion loss of the noise model. Especially in Fig. 12 (b), impedance of the proposed inductor at 200 kHz is much larger than the traditional one; therefore using our proposed method to tune the CM inductors we can achieve higher insertion loss in Fig. 11 at 200kHz. A photo of the proposed CM inductor with the small-space auxiliary winding is shown in Fig. 13. As the impedance network of the auxiliary winding only carries low current high frequency noise, fine wire and low power passive components can be used. Consequently, the size and the footprint area of the tunable CM inductor remain similar to traditional CM inductor.

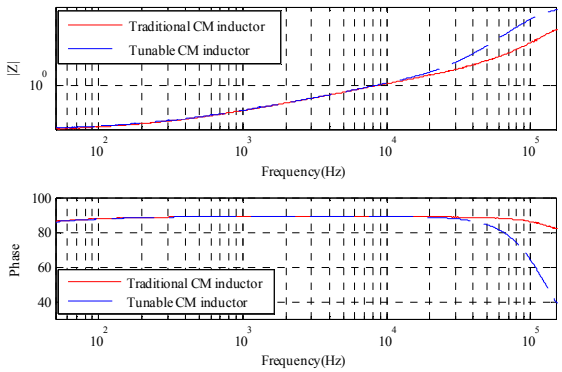

(a)50Hz-150kHz

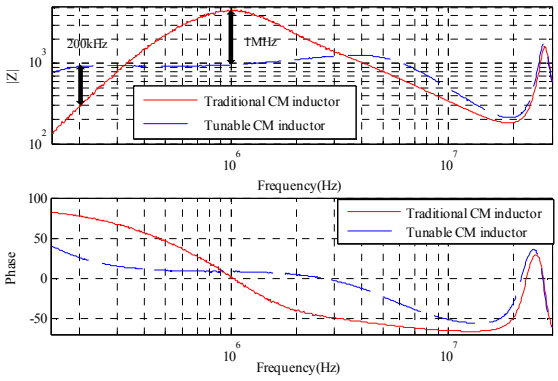

(b) 150kHz-30MHz

Fig. 12. Impedance and phase of the two CM inductors at (a) 50Hz-150kHz and (b) 150kHz-30MHz

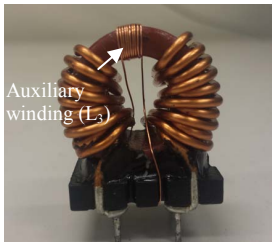

Fig. 13. Photo of the proposed CM inductor

V. CONCLUSION

In this paper, a tunable CM inductor with a small size auxiliary winding is proposed. By connecting an external impedance network to the auxiliary winding, the impedance response of the CM inductor can be altered. This proposed technique is useful in the EMI filter design to eliminate the low frequency resonance between the CM inductor and the parasitic capacitance. This technique is verified by both the analysis and experiment in the design example. Another advantage is the proposed method will not significantly increase the CM inductor power loss. In the practical design, it

may be difficult to determine the parasitic capacitance of the converter because they are related to the printed circuit board and mechanical layout of the converter. In the future work more detailed analysis of the tunable CM inductor will be presented and other auxiliary networks, e.g. other passive and active network will also be explored.

REFERENCES

[1] D. Fu; S. Wang; P. Kong; F.C. Lee; D. Huang; "Novel techniques to suppress the common-mode EMI noise caused by transformer parasitic capacitances in dc-dc converters", IEEE Transactions on Industrial Electronics, Vol.: 60, Issue: 11, 2013, Pages(s) 4968-4977.

[2] M. Pahlevaninezhad; D. Hamza; P.K. Jain; " An Improved Layout Strategy for Common-Mode EMI Suppression Applicable to High-Frequency Planar Transformers in High-Power DC/DC Converters Used for Electric Vehicles", IEEE Transactions on Power Electronics, Vol.: 29, Issue: 3, 2014, Pages(s) 1211-1228.

[3] S. Wang , P. Kong and F. C. Lee "Common mode noise reduction for boost converters using general balance technique", IEEE Trans. Power Electron., vol. 22, no. 4, pp.1410 -1416 2007 .

[4] S. Wang and F. C. Lee; "Analysis and applications of parasitic capacitance cancellation techniques for EMI suppression", IEEE Trans. Ind. Electron., vol. 57, no. 9, pp.3109 -3117 2010

[5] X. Wu; D. Xu; Y. Zhang; Y. Chen; Y. Okuma; K. Mino; " Integrated EMI filter design with flexible PCB structure", In Proc. 2008 Power Electronics Specialists Conference, 2008.

[6] A.J. McDowell; T.H. Hubing; "Parasitic inductance cancellation for surface mount shunt capacitor filters", IEEE Transactions on Electromagnetic Compatibility, Vol.: 56, Issue: 1, 2014, Pages(s) 74-82

[7] S. Wang; C. Xu; "Design theory and implementation of a planar EMI filter based on annular integrated inductor-capacitor unit", IEEE Transactions on Power Electronics, Vol.: 28, Issue: 3, 2013, Pages(s) 1167-1175.

[8] Hsing-Feng Chen; Cheng-Yen Yeh; Ken-Huang Lin "A Method of Using Two Equivalent Negative Inductances to Reduce Parasitic Inductances of a Three-Capacitor EMI Filter", Power Electronics, IEEE Transactions on, On page(s): 2867 - 2872 Volume: 24, Issue: 12, Dec. 2009

[9] S. Wang; Y.Y. Maillet, F. Wang; D. Boroyevich; "Hybrid EMI filter design for common mode EMI suppression in a motor drive system", In Proc. 2008 Power Electronics Specialists Conference, 2008.

[10] M. Ali; E. Laboure; F. Costa; B. Revol; "Design of a hybrid integrated EMC filter for a dc-dc power converter", IEEE Transactions on Power Electronics, Vol.: 27, Issue: 11, 2012, Pages(s) 4380-4390.

[11] J. Biela; A. Wirthmueller; R. Waespe; M.L. Heldwein; K. Raggl; J.W. Kolar; "Passive and active hybrid integrated emi filter", IEEE Transactions on Power Electronics, Vol.: 24, Issue: 5, 2009, Pages(s) 1340-1349.

[12] M. H. Nagrial, A. Hellany, Radiated and Conducted EM1 Emissions in Switch Mode Power Supplies (SMPS): sources, causes and predictions. Proceedings of the IEEE, International Multi Topic Conference, 2001, pp. 54 – 61